Vol. 13: 197–207, 1997 | AQUATIC MICROBIAL ECOLOGY
Aquat Microb Ecol | Published August 21

A simple light meter for measurements of PAR (400 to 700 nm) with fiber-optic microprobes: application for P vs E_0(PAR) measurements in a microbial mat

Michael Kühl[1,*], Carsten Lassen[2], Niels Peter Revsbech[2]

[1]Max Planck Institute for Marine Microbiology, Microsensor Research Group, Celsiusstr. 1, D-28359 Bremen, Germany
[2]Department of Microbial Ecology, Institute of Biological Sciences, University of Aarhus, Ny Munkegade Bldg. 540, DK-8000 Aarhus C, Denmark

ABSTRACT: A simple portable light meter for use with fiber-optic microprobes was developed. The meter has a flat spectral quantum responsivity for 400 to 700 nm light (photosynthetically available radiation, PAR). With scalar irradiance microprobes connected to the meter, it was possible to directly measure photosynthetically available quantum scalar irradiance, E_0(PAR), at <100 µm spatial resolution and over a dynamic range from <1 to >1300 µmol photons m^{-2} s^{-1}. We used the new instrument for scalar irradiance measurements in microbial mats from a freshwater lake (Lake Stigsholm, Denmark) and from a hypersaline pond (Eilat, Israel). Combined measurements of quantum scalar irradiance by fiber-optic microprobes and oxygenic photosynthesis by oxygen microelectrodes made it possible to measure gross photosynthesis as a function of the prevailing scalar irradiance (P vs E_0 curves) at distinct depths within an undisturbed hypersaline microbial mat of immotile unicellular cyanobacteria (*Aphanothece* spp.). Intense photosynthesis by the cyanobacteria resulted in oxygen supersaturation and a 10-fold increase of oxygen penetration in the illuminated mat (z_{max} = 2.5 mm) as compared to the oxygen penetration in dark incubated mats (z_{max} = 0.2 to 0.3 mm). The mat changed from a net oxygen consuming to a net oxygen producing community at an oxygen compensation irradiance of 14 to 26 µmol photons m^{-2} s^{-1}. The photic zone of the microbial mat was only 0.6 mm deep due to a high attenuation of PAR. The diffuse vertical attenuation coefficient of E_0(PAR) was K_0(PAR) = 6.3 mm^{-1}. In the upper 0.2 mm of the microbial mat photosynthesis was photoinhibited at scalar irradiance above 200 µmol photons m^{-2} s^{-1}. At 0.3 mm the strong light attenuation prevented inhibition in deeper layers of the microbial mat and photosynthesis approached saturation at 35 µmol photons m^{-2} s^{-1}. In the lower part of the photic zone, photosynthesis increased linearly with E_0(PAR). Areal gross photosynthesis exhibited no photoinhibition at high irradiance and started to approach saturation above a downwelling quantum irradiance of 97 µmol photons m^{-2} s^{-1}.

KEY WORDS: Light penetration · Photosynthesis · Scalar irradiance · Microbial mat · Cyanobacteria · Photoinhibition · Microsensor · Light meter · Calibration

INTRODUCTION

In photosynthetic sediments, biofilms and microbial mats, light penetrates only a few mm due to strong scattering and absorption by the dense matrix of mineral grains, exopolymers and pigment-containing microorganisms. With fiber-optic microprobes, it is possible to measure depth profiles of various light field parameters at 50 to 100 µm spatial resolution (see e.g. review by Kühl et al. 1994b), which can then be related to the depth distribution of photosynthesis and the chemical microenvironment measured at same scale by microelectrodes in mats and sediments (Revsbech 1994).

A simple set-up for measurements of spectral field radiance, $L(\lambda; \theta, \phi)$, i.e. the quantum flux per unit area per unit solid angle from a defined direction, (θ, ϕ), in a

*E-mail: michael@postgate.mpi-mm.uni-bremen.de

spherical coordinate system, was described by Jørgensen & Des Marais (1986), who coupled a tapered optical fiber to a single battery-operated photodiode. With this set-up it was possible to study spectral light penetration in microbial mats by inserting interference filters (half bandwidth, HBW, of 15 to 30 nm) in front of the light source while measuring depth profiles of downwelling radiance. By measuring radiance profiles at various angles relative to the incident light, the spectral scalar irradiance, i.e., the spherical integrated quantum flux from all directions about a point, $E_0(\lambda) = \int_{4\pi} L(\lambda; \theta, \phi)d\omega$, at various depths could also be calculated (Jørgensen & Des Marais 1988). A similar set-up equipped with a 420 to 730 nm transmission filter was used by Dodds (1992) to estimate integral 400 to 700 nm photon scalar irradiance, E_0(PAR) (PAR = photosynthetically available radiation), in periphytic biofilms with a 250 µm thick optical fiber coated with diffusing material at its light collecting end. Due to non-ideal light collecting properties and a variable quantum responsivity of the photodiode detector system over the spectral range measured, measurements at several orientations of the probe were, however, still necessary and required a relatively complicated calibration procedure in order to estimate the scalar irradiance.

Lassen et al. (1992a) developed a fiber-optic microprobe with an isotropic angular response for incident VIS-NIR (visible, near-infrared) light. A similar microprobe was developed by Garcia-Pichel (1995) for spectral measurements of UV-VIS (ultra-violet, visible) light. With these microprobes it is possible to directly measure scalar irradiance, which especially in benthic environments is the most relevant measure of light available for photosynthesis (Smith & Wilson 1972, Højerslev 1981, Kühl et al. 1994a). Recently, fiber-optic microprobes for irradiance, $E_d(\lambda) = \int_{2\pi} L(\lambda; \theta, \phi)\cos(\theta)d\omega$, i.e. the downwelling quantum flux per unit horizontal surface area, were also developed (Kühl et al. 1994a, Lassen & Jørgensen 1994).

The light-scattering material covering the sensor tip decreases the amount of light collected by the irradiance and the scalar irradiance fiber probes by 2 to 3 orders of magnitude relative to the amount of light collected by a bare untapered fiber probe in a collimated light beam incident at 0° zenith angle (Lassen et al. 1992a, Garcia-Pichel 1995). Although the small transmittance of the sphere material is partly compensated by the much larger acceptance angle of the scalar irradiance probe as compared to a radiance probe, light measurements with irradiance or scalar irradiance microprobes require a detector with >10- to 100-fold higher sensitivity than the simple photodiode detector described by Jørgensen & Des Marais (1986).

An intensified diode array spectral detector system for use with fiber-optic microprobes was described by Kühl & Jørgensen (1992). The high sensitivity of the system enables high spectral resolution (3 to 5 nm HBW) light measurements with fiber-optic microprobes (e.g. Lassen et al. 1992b, Kühl et al. 1994b) but this type of detector system is expensive and difficult to transport. In most ecological studies light available for photosynthesis (PAR) is measured with large broad band quantum sensors, which integrate light from 400 to 700 nm (Jewson et al. 1984, Kirk 1994). Comparable simple instrumentation for microscale PAR measurements is to our knowledge not available. We describe here a simple portable instrument for PAR measurements with fiber-optic scalar irradiance microprobes and demonstrate its application for light and photosynthesis studies in a microbial mat.

MATERIALS AND METHODS

Description of PAR meter. A fiber-optic scalar irradiance microprobe was coupled via a SMA type optical fiber connector to a photomultiplier tube (PMT, Oriel 77344, Oriel Corp., USA) with a wavelength range from 160 to 930 nm and a relativly flat spectral quantum responsivity. The PMT was mounted in a black housing and a set of filters was placed in a unit between the PMT and the connector. A short-pass filter (Oriel 58891) with a cut-off slope at 700 nm of < 3% blocked light up to 985 nm. A long-pass glass-plastic filter (Schott KV 399, Germany) blocked light below 400 nm. The PMT, optical filters and the necessary electronics for operation of the PMT (high voltage and regulating voltage supply, and voltage divider) were mounted in a small box that operates with 6 to 12V DC external voltage from e.g. a battery (Fig. 1A). The detector electronics allowed for simple adjustment of the PMT sensitivity, i.e. via adjustment of the PMT high voltage, suppression of the PMT dark current, and converted the current generated by photoelectrons in the PMT to an analogue output signal, which was acquired by a personal computer equipped with an A/D card and controlled by a home-made Pascal program. All the main components of the PAR meter are commercially available, relatively inexpensive and require only a minimum of electronic and mechanical adaptation in order to have a functioning instrument.

Spectral responsivity and linearity. The relative spectral response of the PAR instrument was determined at 10 nm steps from 400 to 730 nm by inserting discrete interference filters (Oriel Corp., HBW 10 to 15 nm) in the light path between the light source and the microprobe (Fig. 2A). The light source was a fiber-optic tungsten halogen lamp equipped with a collimat-

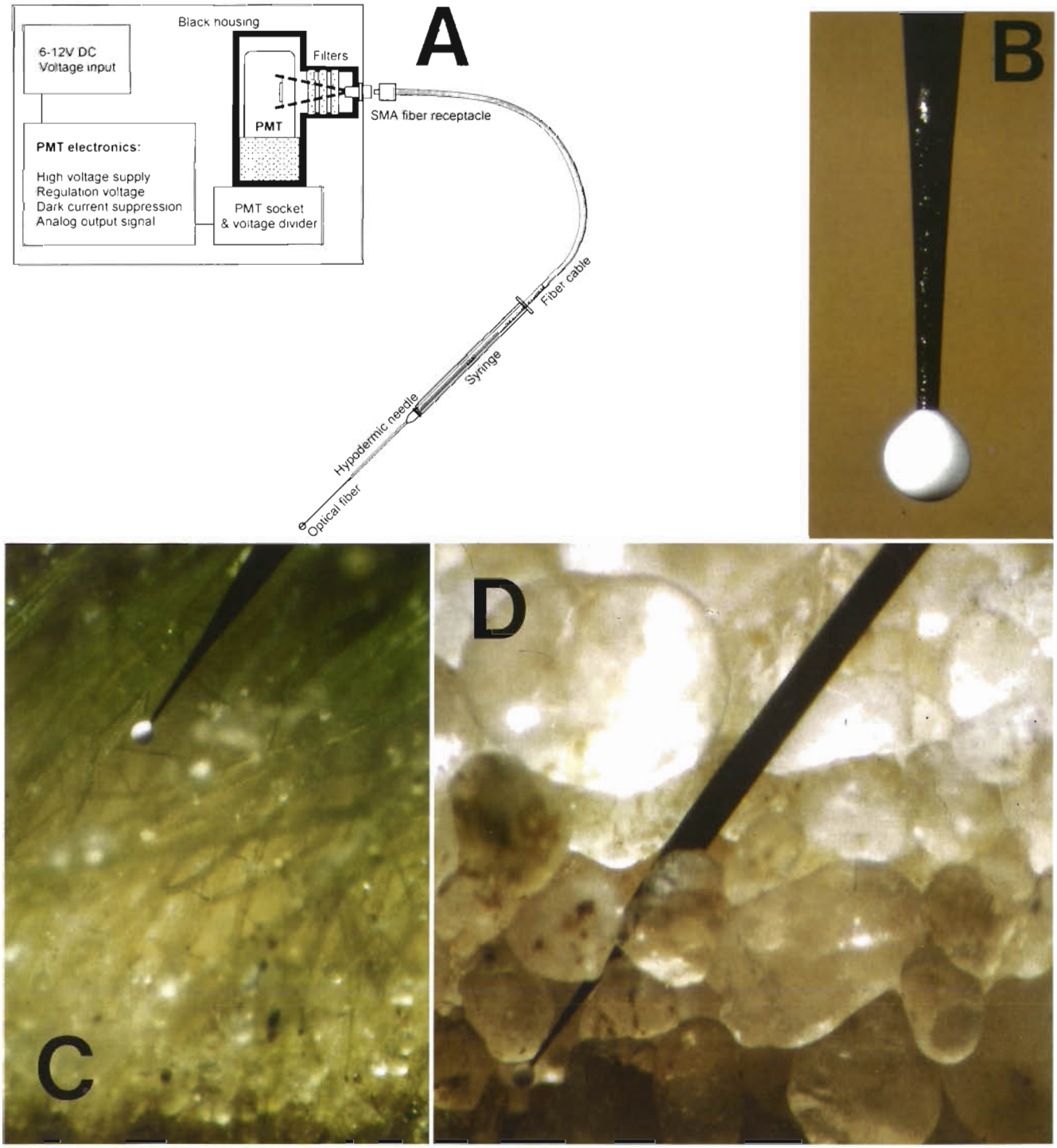

Fig. 1. (A) Schematic drawing of the new system for microscale PAR measurements. Fiber-optic microprobes are connected to the system via standard SMA fiber-optic connectors. (B) Tip of a scalar irradiance microprobe. (C, D) A scalar irradiance microprobe inserted into a community of filamentous green algae and a sandy sediment, respectively. The scattering sphere at the tapered fiber tip has a diameter of ca 80 µm

ing lens (Schott KL-1500). The absolute quantum irradiance of each waveband was measured simultaneously with another fiber-optic microprobe connected to a detector system (O-SMA, Spectroscopy Instruments) consisting of a spectrograph (Jarrel Ash, Monospec 18) and an optical multichannel analyser (Princeton Instruments, EIRY-1024) (Kühl & Jørgensen 1992). This detector system was previously calibrated by a spectral

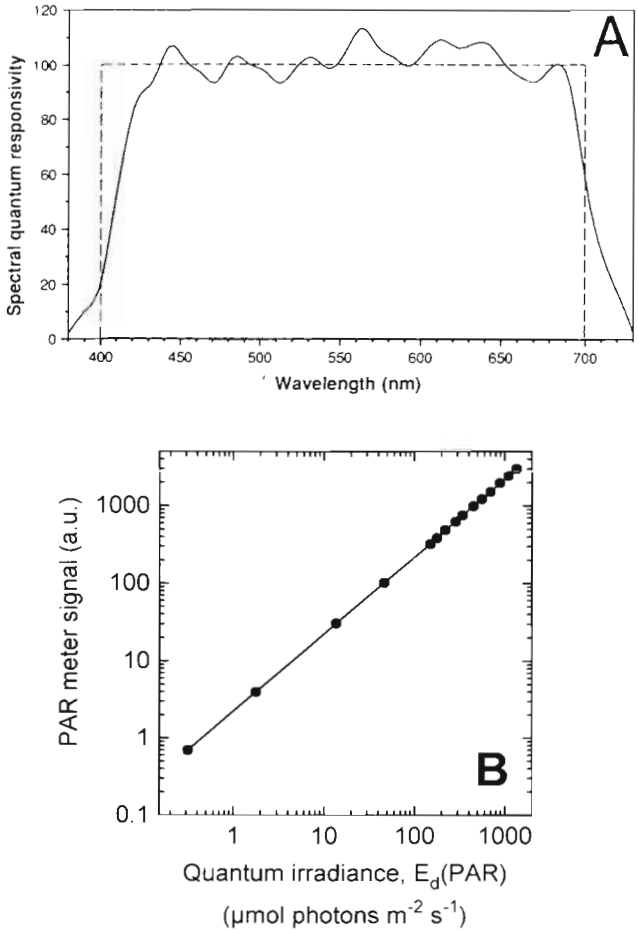

Fig. 2. (A) Relative spectral quantum responsivity of the detector system equipped with a scalar irradiance microprobe (solid line). Dashed line: ideal response function for a PAR quantum meter. (B) PAR (400 to 700 nm) response of the detector system measured underwater in a collimated light beam at various downwelling quantum irradiance values. The linearity of the new detector system was checked by linear regression, yielding a correlation coefficient of $r^2 > 0.999$ (n = 15)

irradiance quartz tungsten-halogen calibration lamp (Oriel 6333) (Lassen et al. 1992b). The fiber-optic microprobes for scalar irradiance used in this study were made according to Lassen et al. (1992a) and consisted of a small diffusing sphere (<100 µm diameter) cast at the tip of a tapered optical fiber coated with chromium and black enamel paint (Fig. 1B, C). The PMT equipped with the short- and long-pass filters previously mentioned resulted in a nearly flat spectral quantum responsivity curve of the PAR meter over the 400 to 700 nm wavelength range, and it was not necessary to add colour-compensating filters (Fig. 2A).

The linearity of the instrument (fiber-optic microsensor and detector unit) for a given PMT voltage was checked by inserting neutral density filters (Oriel Corp.) with a known transmission in the light path between the collimated light source and the microprobe. For each neutral density filter combination, the light intensity signal (corrected for the dark signal of the instrument) was measured underwater with a scalar irradiance microprobe connected to the PMT detector unit and also with an underwater quantum irradiance meter (LiCor, USA). The results showed a linear response of the new instrument from >1300 µmol photons m^{-2} s^{-1} down to a scalar irradiance of <0.5 µmol photons m^{-2} s^{-1} (Fig. 2B). Thus a simple 2 point calibration of the detector response in water at a known downwelling irradiance and in darkness was sufficient for microscale *xyz*(PAR) measurements in units of µmol photons m^{-2} s^{-1}.

Measurements in a microbial mat. We used the new detector system for measuring E_0(PAR) and photosynthesis in a hypersaline cyanobacterial mat growing in an artificial salt pond at the H. Steinitz Marine Laboratory, Interuniversity Institute, Eilat, Israel. Mat samples were taken with black Plexiglas core tubes and carefully transferred to a small flow chamber where aerated brine was continuously flowing over the mat. The brine salinity was 100‰ and the temperature was 21 to 22°C. The relatively smooth surface layer of the mat was dominated by a dense ca 1 mm thick brownish-green layer of unicellular cyanobacteria (*Aphanothece* spp.) in an exopolymer matrix and some filamentous cyanobacteria (*Phormidium* spp., *Microcoleus* spp.) on top of the underlying reduced mat, where colourless sulfur bacteria (*Beggiatoa* sp.) were abundant. The mat was illuminated vertically from above with collimated light from a fiber-optic halogen lamp (Schott KL-1500). Different light intensities were achieved by inserting neutral density filters with a known transmittance (Oriel Corp.) in the light path between light source and mat surface. The downwelling 400 to 700 nm quantum irradiance for each filter combination was measured by an underwater quantum irradiance meter (LiCor) placed at the same distance and position relative to the light source as the surface of the microbial mat. Downwelling quantum irradiance (= the downwelling quantum scalar irradiance in a collimated light beam) was also measured by the new PAR meter with the tip of a scalar irradiance microprobe placed over a black light well, which was placed at the same distance and position relative to the light source as the surface of the microbial mat (Lassen et al. 1992b).

Depth profiles of oxygen concentration were measured by Clark-type oxygen microelectrodes (Revsbech 1989) connected to a custom built pA meter. Oxygenic photosynthesis was measured by the light-dark shift method for gross photosynthesis (Revsbech & Jørgensen 1983). The oxygen microelectrodes (tip diameter of 5 to 15 µm) had a response time of 0.2 to 0.4 s, a stirring sensitivity of <1 to 2%, and exhibited a measuring current of

0 to 2 pA in anoxic water and 150 to 250 pA in air saturated water. Both oxygen and scalar irradiance measurements were done with the microsensors mounted on a motorised micromanipulator (Märtzhäuser, Germany). Depth profiles were measured at a zenith angle of 135° relative to the vertically incident light. Measuring signals from the pA meter and the new PAR meter were recorded both on a strip chart recorder and on a computer equipped with an A/D card and controlled by a custom-made Pascal software. The computer and software also controlled the motorised micromanipulator.

RESULTS AND DISCUSSION

Evaluation of PAR meter

In order to evaluate the performance of the new PAR meter, we compared data obtained with the new meter with PAR data obtained with a calibrated spectral detector system. Spectral scalar irradiance measurements were done in sediment collected in small Plexiglas core tubes from a small eutrophic shallow water lake, Lake Stigsholm, Denmark (Fig. 3). The measurements were done with a scalar irradiance microprobe connected to the spectral detector system (O-SMA) as described earlier (Kühl & Jørgensen 1992). The sediment was covered by a dense flocculent layer of benthic green algae (*Oedogonium* spp. and *Pediastrum* sp.) and smaller amounts of diatoms. The scalar irradiance spectra showed clear minima at major absorption wavelengths of chl *a* (675 nm) and chl *c* (620 to 630 nm). Blue light at 400 to 550 nm exhibited the strongest attenuation due to chlorophyll and carotenoid absorption and <0.1% of the incident blue light was found 3 mm below the sediment surface. Infrared light was attenuated much less with depth. Below 3 mm depth NIR light intensities were 2 to 3 orders of magnitude higher than in the visible part of the spectrum. The response of a photon scalar irradiance PAR meter can be expressed as (Lassen et al. 1992b):

$$E_0(\mathrm{PAR}) = C \int_{\lambda=400}^{700} \int_{4\pi} L(\lambda; \theta, \phi)(\lambda/hc)\, F(\lambda)\, F(\omega)\, d\lambda d\omega \quad (1)$$

where $F(\lambda)$ is the spectral response function, $F(\omega)$ is the directional response function of the scalar irradiance sensor, and C is a calibration constant (in practice determined by relating measurements in a uniform collimated light beam with a calibrated irradiance meter to the signal recorded by the new measuring system equipped with a scalar irradiance microprobe; Fig. 2B). $L(\lambda, \theta, \phi)$ is the spectral field radiance, and the term (λ/hc) converts units from energy equivalents to photons by multiplication with the ratio of the wavelength, λ, to the product of Planck's constant, h, and the velocity of light *in vacuo*, c (Kirk 1994).

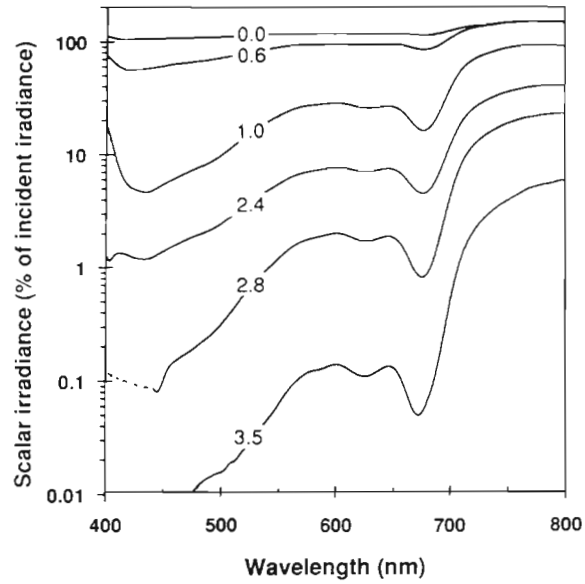

Fig. 3. Spectral scalar irradiance in a green algal mat (*Oedogonium* spp. and *Pediastrum* sp.) from Lake Stigsholm, Denmark. Numbers on curves indicate the depth in mm below the mat surface. Data were normalised to the incident downwelling irradiance at the mat surface

Importance of non-ideal isotropic response

Fiber-optic scalar irradiance microprobes consist of a tapered fiber with a light-scattering sphere cast on the tip. While a perfect scalar irradiance meter integrates light from all directions equally, the actual microprobe has a blind spot, where the fiber enters the sphere (Fig. 1B). The fiber connection comprises, however, <2% of the whole surface area of the sphere (Lassen et al. 1992a). The typical directional response of a scalar irradiance microprobe connected to the present PAR meter was isotropic (±10%) for incident light from −160° to +160° (Lassen et al. 1992a, Kühl et al. 1994a). Such small deviations of $F(\omega)$ from a perfectly isotropic response lead to a small error (1 to 2%) in the determination of E_0(PAR) with large scalar irradiance detectors in water (Booth 1976). The anisotropy of the radiance distribution in water is much more pronounced compared to the radiance distribution in sediments and biofilms (Kühl & Jørgensen 1994). We assume that the error from the relatively small deviation in isotropic response of our system will partially be smoothed out by the highly diffuse light field in the sediment and can therefore be ignored. Further evaluation of this assumption would require detailed measurements of the radiance distribution with field radiance microprobes (Kühl & Jørgensen 1994, Kazarinova-Fukshansky et al. 1996, N. Kazarinova-Fukshansky, L. Fukshansky, M. Kühl & B.

B. Jørgensen unpubl.) in combination with scalar irradiance measurements with the new PAR meter. A first approximation of the error was, however, calculated from previously published radiance distributions for 650 nm light measured in sediments and measured acceptance functions for a scalar irrradiance microprobe (Kühl & Jørgensen 1994, Kühl et al. 1994b) following a method originally decribed by Booth (1976).

Measured radiance distributions measured at equidistant angular intervals and corrected for the non-uniform angular sensitivity of the field radiance microprobes (Kazarinova-Fukshansky et al. 1996) were used to calculate scalar irradiance as

$$E_0 = \sum_{\theta=0^\circ}^{180^\circ} L_\theta w_\theta \quad (2)$$

where L_θ denotes the field radiance measured in a direction specified by the zenith angle, θ, relative to the vertically incident collimated light beam and representative for all azimuthal directions around the vertical axis, i.e. a spherical band specified by the measuring direction, θ, and the acceptance angle of the field radiance microprobe (±10°) (see Kühl & Jørgensen 1994 and Kazarinova-Fukshansky et al. unpubl. for more details). The weighting factor, w_θ, equals the fractional area of the individual bands on a unit sphere ($\sum_\theta w_\theta = 4\pi$). The error introduced by using a scalar irradiance probe with imperfect isotropic response can then be approximated from the ratio of the scalar irradiance measured by a real sensor and an ideal sensor, respectively (assuming azimuthal symmetry of both the light field and the sensor acceptance function):

$$R = C \frac{\sum_{\theta=0^\circ}^{180^\circ} L_\theta w_\theta F_\theta}{\sum_{\theta=0^\circ}^{180^\circ} L_\theta w_\theta} \quad (3)$$

where F_θ denotes the relative response of a scalar irradiance microprobe in the direction θ, here F_θ is normalized so that $\overline{F_\theta}|_\theta = 1$. For a perfect isotropically responding scalar irradiance sensor $F_\theta = 1$ for all θ. The normalization factor, C, is selected so that $R = 1$ in the case of a totally isotropic light field, where all L are equal (Booth 1976).

We calculated R with 3 different radiance distributions measured in clean quartz sand, in coastal sediment with diatoms, and in a coastal sediment with a dense cyanobacterial mat, respectively (Table 1). For each sediment type the most anisotropic radiance distribution at the sediment surface as well as the more diffuse radiance distribution within the sediment was considered. As expected, we found the highest deviations due to imperfect angular response of the scalar irradiance probe in the most anisotropic light fields at the sediment surface. The highest deviations were found in the microbial mat, where the radiance distribution remained relatively anisotropic with depth (cf. Kühl et al. 1994b). The magnitude of the error in all investigated cases was, however, negligible in comparison to other uncertainties in the practical application of scalar irradiance microprobes. Our analysis assumes azimuthal symmetry of light fields and acceptance function of the microprobe for a given orientation of the probe. This may result in an underestimation of the error involved. Until a more detailed analysis has been undertaken, a conservative estimate of the maximal error due to imperfect isotropic response probably lies around 2 to 5%.

Importance of non-ideal spectral response

The non-ideal spectral responsivity, $F(\lambda)$, of the PAR meter was evaluated by calculating depth profiles of E_0(PAR) from the spectral data in Fig. 3 using Eq. (1) (Fig. 4). This was done with the actual measured spectral responsivity of the PAR instrument (Fig. 2A, solid curve) and compared to E_0(PAR) profiles calculated from the spectral data, assuming an ideal flat spectral responsivity (Fig. 2A, dashed curve). The actual PAR instrument spectral responsivity results in a slight overestimation (<10 to 15%) of measured E_0(PAR) as compared to a perfect PAR meter throughout most of the sediment. At E_0(PAR) intensities <2 to 3% of the

Table 1. Directional response function for a scalar irradiance microprobe calculated for different radiance distributions and probe orientations

Radiance distribution	Directional response, R (mean ± SD)[c] (n = 18)
Wet quartz sand[a]	
0.0 mm	1.00770 ± 0.04504
0.5 mm	1.00003 ± 0.01635
1.0 mm	0.99993 ± 0.01799
Sediment + diatoms[a]	
0.0 mm	1.00110 ± 0.06457
0.5 mm	1.00031 ± 0.02498
1.0 mm	1.00006 ± 0.01569
Microbial mat[b]	
0.0 mm	1.00216 ± 0.05760
0.5 mm	1.00018 ± 0.01696
1.0 mm	1.00051 ± 0.01699
Isotropic	1.00000

[a]Kühl & Jørgensen (1994), [b]Kühl et al. (1994b)
[c]Calculated from Eq. (3) by mathematically rotating the scalar irradiance microprobe in steps of 10° in the light field assuming azimuthal symmetry of both radiance distribution and acceptance function of the microprobe

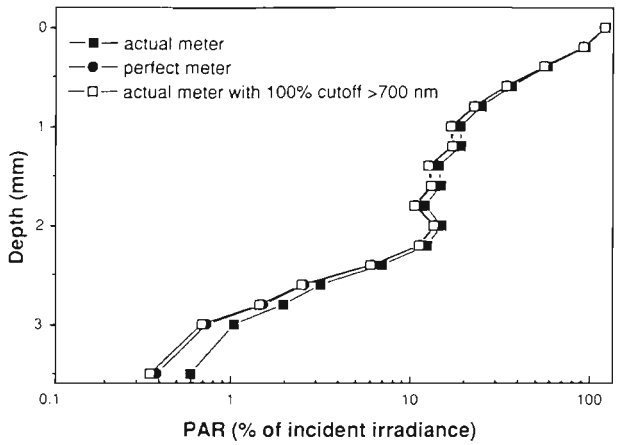

Fig. 4. Depth profiles of 400 to 700 nm quantum scalar irradiance (PAR) calculated from spectral measurements in a green algal mat from Lake Stigsholm, Denmark (Fig. 3). (●) Calculated assuming perfectly flat response from 400 to 700 nm; (■) calculated with actual PAR meter responsivity; (□) calculated with PAR meter responsivity assuming 100% cut-off of light >700 nm. Data were normalised to the downwelling 400 to 700 nm quantum irradiance at the mat surface

incident light this overestimation became significantly higher (25 to 50%) (Fig. 4). Depth profiles of E_0(PAR) calculated with the actual responsivity curve but assuming a 100% cut-off at 700 nm were, however, almost identical to the E_0(PAR) profiles calculated for a perfect PAR meter. The overestimation of E_0(PAR) by the new instrument thus was primarily due to the non-ideal cut-off at 700 nm. Even though the spectral responsivity of the meter decreases from 60% at 700 nm to <5% at 730 nm (Fig. 2A), the observed increase of the relative amount of NIR light in comparison to PAR in deeper sediment layers (Fig. 3) could easily account for the observed overestimation of E_0(PAR) with the present meter.

In water these effects of NIR light would be insignificant due to the efficient absorption of NIR light by water and the 10^2- to 10^5-fold lower attenuation coefficients of PAR found in planktonic environments compared to benthic environments (Kirk 1994). A high attenuation of PAR combined with a lower attenuation of NIR light is, however, a general observation in benthic environments. Table 2 shows a compilation of scalar

Table 2. Scalar irradiance attenuation coefficients, K_0, of visible (PAR, 400 to 700 nm) and near-infrared radiation (NIR, 700 to 880 nm) measured in microbial mats and sediments from various localities in Denmark, France and Israel

	Depth (mm)	Grain size (µm)	K_0(PAR) (mm^{-1})	K_0(NIR) (mm^{-1})	Photic zone (mm)
Sandy sediments					
Pure quartz sand[a]	Asymptotic	<63	3.4	2.8	
	Asymptotic	63–125	1.6	1.4	
	Asymptotic	125–250	1.6	1.2	
	Asymptotic	250–500	1	0.8	
Limfjorden[b]	0.0–1.0	125–250	1.2	–	2.7
	1.0–2.0		1.5	–	
Kalø Vig[c]	0.0–1.0	125–250	1.3	–	2.2
	1.0–2.0		1.7	–	
Limfjorden, cyanobacterial mat[d]	0.0–0.6	125–250	3.3	–	1.0
	0.6–1.2		2.6	–	
Lake Stigsholm (this study)	0.0–1.0	63–125	1.8	–	2.0
	1.0–3.0		2.2	–	
Lake Stigsholm, green algal flocs	0.0–1.0	63–125	1.4	–	2.4
	1.0–3.0		1.9	–	
Ile aux Oiseaux[e]	0.0–1.0	125–250	1.0	–	1.6
	1.0–2.0		1.6	–	
Etang de Prevost[e]	0.0–1.0	125–250	2.6	1.8	0.9
	1.0–2.0		3.8	3.5	
Pointe de la Coubre[f]	0.0–0.6	125–250	9.9	5.6	0.3
Silty sediments and microbial mats					
Certez, uncolonized[e]	0.0–0.6	<63	8.8	6.3	0.0
Certez, diatoms[e]	0.0–0.6	<63	2.7	2.2	0.8
	0.6–1.2		5.0	4.2	
Certez, *Oscillatoria* mat[e]	0.0–0.6	<63	11.7	2.6	0.6
Certez, *Anabaena* mat[e]	0.0–0.6	<63	3.9	–	0.7
	0.6–1.2		6.5	–	
Skødstrup, *Oscillatoria* biofilm[g]	0.0–0.6	–	4.7	–	0.6
Eilat, *Aphanothece* mat (this study)	0.0–0.6	–	6.3	–	0.6

[a]Kühl et al. (1994a), [b]Lassen et al. (1992b), [c]Kühl & Jørgensen (1992), [d]Ploug et al. (1993), [e]Lassen et al. (1994), [f]Lassen & Jørgensen (1994), [g]Kühl et al. (1996)

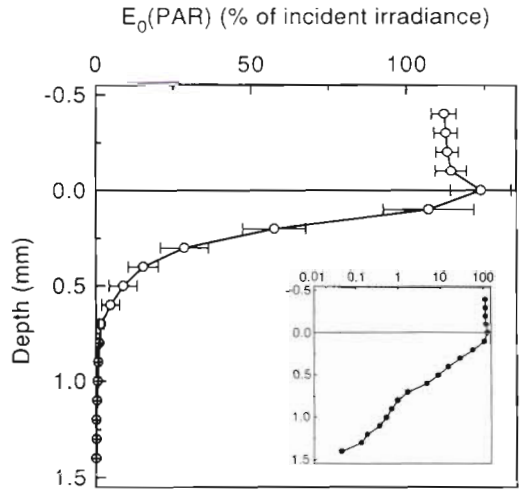

Fig. 5. Depth profile of photon scalar irradiance, E_0(PAR), in a hypersaline microbial mat, Eilat, Israel. Data were normalised to the downwelling photon irradiance at the mat surface. Symbols and error bars represent the mean and standard deviation of 8 measurements, respectively. Inset shows the same data using a log scale for the light intensity

irradiance attenuation coefficients of PAR and NIR light measured in various sediments. The highest differences between PAR and NIR attenuation coefficients are found in optically dense microbial mats with a photic zone of <1 mm (Table 2). The performance of the new PAR meter can probably be improved further by selecting a short-pass filter with a steeper cut-off around 700 nm. In comparison to large PAR quanta meters the present meter has, however, a similar or even better spectral responsivity [compare e.g. with Jerlov & Nygaard 1969, Biggs (LiCor Inc. application note), Biggs et al. 1971, Booth 1976, Spitzer & Wernand 1979], and the present meter allows for reliable PAR measurements down to ca 1% of the incident quantum irradiance, i.e. throughout the euphotic zone for oxygenic photosynthesis in most microbenthic communities.

PAR, photosynthesis and oxygen microprofiles in a microbial mat

The depth distribution of photon scalar irradiance in the cyanobacterial mat is shown in Fig. 5. Photon scalar irradiance, E_0(PAR), reached up to 125% of the incident photon irradiance at the microbial mat surface, and at 0.1 mm depth E_0(PAR) was still >100 to 105% of the incident irradiance. The presence of a near-surface maximum of scalar irradiance is commonly observed in microbenthic communities and the physical background for this phenomenon is discussed elsewhere (Kühl & Jørgensen 1994). Within the microbial mat E_0(PAR) was attenuated exponentially with depth to <1% of the incident irradiance at 0.7 mm and to <0.1% at 1.4 mm depth (Fig. 5). The attenuation coefficient for photon scalar irradiance, K_0(PAR), within the photic zone was calculated as $K_0(\mathrm{PAR}) = -\mathrm{d}\ \ln E_0(\mathrm{PAR})/\mathrm{d}z = 6.3\ \mathrm{mm}^{-1}$, by a linear regression on ln-transformed data over the 0.1 to 0.6 mm depth interval ($r^2 > 0.99$) (Kühl & Jørgensen 1994). The attenuation coefficient lies within the range of K_0(PAR) attenuation coefficients we found in other microbial mats (Table 2).

Oxygen penetration into the mat increased 10-fold from ca 0.2 to 0.3 mm in the dark to ca 2.5 mm at an incident quantum irradiance of 1355 µmol photons m^{-2} s^{-1} (comparable to full daylight), and highest oxygen concentrations in the mat were almost 6 times higher than in the overlying air-saturated water (Fig. 6A). The most dramatic increase of oxygen penetration depth and oxygen concentration in the mat occurred at the lowest irradiances, and at incident irradiances >340 µmol photons m^{-2} s^{-1} the oxygen profiles were almost identical (Fig. 6B). The mat changed from a net oxygen consuming community to an oxygen producing community at an incident irradiance between 14 and 26 µmol photons m^{-2} s^{-1} (Fig. 6B). Due to the strong light attenuation within the mat, the bottom of the euphotic zone was found at 0.6 mm depth at an incident quantum irradiance of 1356 µmol photons m^{-2} s^{-1}

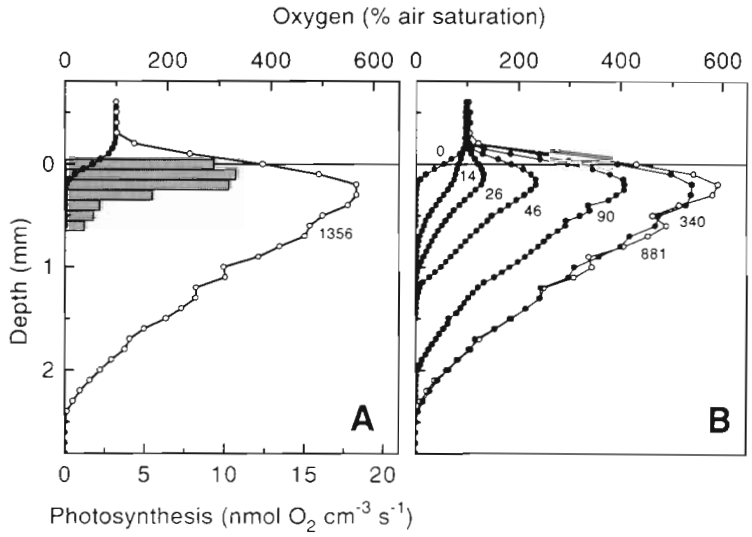

Fig. 6. Depth profiles of oxygen and oxygenic photosynthesis in a cyanobacterial mat. (A) Oxygen profiles in the dark (●) and at high light intensity (○). Shaded bars indicate the photosynthetic rate. (B) Depth distribution of oxygen at increasing light intensities. Numbers on curves indicate the incident quantum irradiance in µmol photons m^{-2} s^{-1} at the mat surface

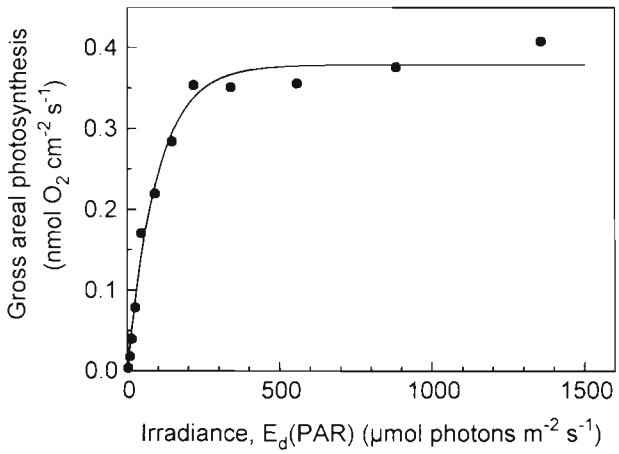

Fig. 7. Areal gross photosynthesis (●) of a cyanobacterial mat as a function of incident quantum irradiance, E_d(PAR). An exponential model (Webb et al. 1974, more details in the text) was fitted to the P vs E_d(PAR) curve (solid line, $r^2 > 0.98$). Curve fitting was done with a non-linear regression Levenberg-Marquardt algorithm (Origin 3.0, MicroCal Software Inc.)

(Fig. 6A), where E_0(PAR) was attenuated to <5% of the incident irradiance at the mat surface (Fig. 5).

Total areal gross photosynthesis of the mat increased strongly with light intensity and started to become saturated above an incident irradiance of ca 200 µmol photons m^{-2} s^{-1} (Fig. 7). At higher irradiances photosynthesis continued to increase slowly and no photoinhibition of gross areal photosynthesis was found. From a fit of an exponential model (see below) to the P vs E_d curve (solid line in Fig. 8) a maximal areal gross photosynthetic rate of $P_{g,max}$ = 0.378 nmol O_2 cm^{-2} s^{-1} and an onset of light saturation of areal gross photosynthesis at an irradiance of I_k = 97 µmol photons m^{-2} s^{-1} was calculated.

The gross photosynthetic activity at different depths plotted against the prevailing scalar irradiance measured at the same depths demonstrated, however, different patterns of photosynthetic performance throughout the photic zone of the microbial mat (Fig. 8). In the upper 0.0 to 0.1 mm of the mat gross photosynthesis was photoinhibited above a scalar irradiance of 300 µmol photons m^{-2} s^{-1}. We fitted an exponential formulation for P vs I curves including photoinhibition to our data from 0.1 mm depth (Platt et al. 1980):

$$P(z) = P_s(z)\left[1 - \exp(-aE_0(\mathrm{PAR}))\right]\exp(-bE_0(\mathrm{PAR})) \quad (4)$$

where $P(z)$ and E_0(PAR) are the gross photosynthesis and the photon scalar irradiance at depth, z, respectively; $P_s(z)$ is the maximal photosynthetic rate observed; $a = \alpha/P_s$, and $b = \beta/P_s$, i.e. the ratio of the initial slope, α, and the slope of the photoinhibited part of the P vs I curve, β, over P_s, respectively. The curve fit ($r^2 > 0.99$) resulted in P_s(0.1 mm) = 12.90 µmol O_2 cm^{-3} s^{-1}, α = 0.173, and β = 0.002.

At 0.3 mm depth, the strong light attenuation in the mat prevented photoinhibition, and gross photosynthesis exhibited saturation above a scalar irradiance of ca 100 µmol photons m^{-2} s^{-1}. For this depth, we fitted the exponential model (Webb et al. 1974, Geider & Osborne 1992):

$$P(z) = P_m(z)\left[1 - \exp\left(-\alpha\frac{E_0(PAR)}{P_m(z)}\right)\right] \quad (5)$$

to our data, where $P_m(z)$ is the maximum rate of light saturated photosynthesis, and α is the initial slope of the P vs E_0(PAR) curve. The curve fit ($r^2 > 0.98$) yielded a P_m(0.3mm) = 5.06 nmol O_2 cm^{-3} s^{-1} and an initial slope α = 0.144. The scalar irradiance at the onset of light saturation, I_k, could then be calculated as $I_k = P_m/\alpha$ = 35.1 µmol photons m^{-2} s^{-1} for photosynthesis at 0.3 mm depth in the mat.

In the lower part of the photic zone, at depths below 0.4 to 0.5 mm, photosynthesis increased linearly with scalar irradiance and no saturation curve was observed within the range of incident irradiances applied in the experiment (data not shown).

Various formulations of P vs I curves are described in the literature (see e.g. Chapter 7 in Geider & Osborne 1992). Besides the exponential models shown in Eqs. (4) & (5), the hyperbolic tangent function of Jassby & Platt (1976), $P(z) = P_m \tanh(\alpha E_0(\mathrm{PAR})/P_m)$, is the most popular model used to describe P vs I curves of aquatic photosynthesis. We also fitted this function to our data

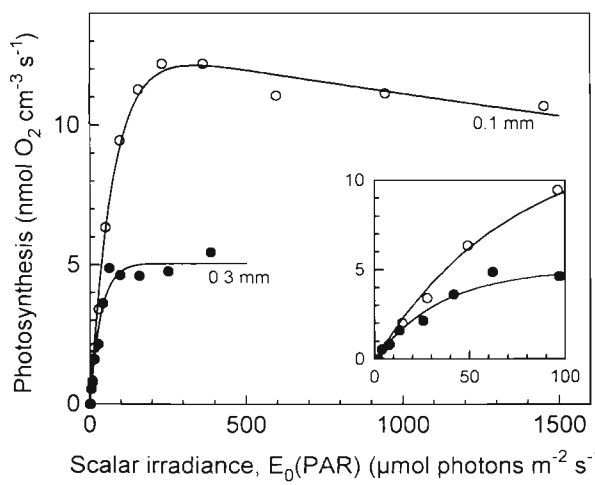

Fig. 8. Gross photosynthesis vs quantum scalar irradiance, E_0(PAR), at 2 depths in a cyanobacterial mat (depth indicated as numbers on graph). Solid lines: fits of the exponential model of Platt et al. (1980) formulated for P vs I curves with photoinhibition (0.1 mm depth, $r^2 > 0.99$) and without photoinhibition (0.3 mm depth, $r^2 > 98$). Curve fitting was done with a non-linear regression Levenberg-Marquardt algorithm (Origin 3.0, MicroCal Software Inc.). The inset shows a more detailed picture of the same dataset in the low light region of the P vs E_0(PAR) curves

from 0.3 mm but did not find a significantly better fit ($r^2 > 0.98$, data not shown). The hyperbolic tangent is a purely empirical function, while the formulation of the exponential model is mathematically identical to the target theory describing photosynthesis yield as a function of irradiance at the level of the photosynthetic apparatus (Eilers & Peeters 1989, Geider & Osborne 1992, Baumert 1996). Currently, we therefore prefer the exponential model but there is a strong need for a detailed investigation of P vs I curves and their mathematical formulation in microbenthic environments. Most data and modelling approaches of P vs I curves in aquatic systems relate to phytoplankton, macroalgae and macrophyte photosynthesis (Kirk 1994, Geider & Osborne 1992, and references therein), while a systematic study of microbenthic photosynthesis is still lacking.

Another complication for the interpretation of microscale photosynthesis measurements yet to be solved is the sensitivity of the light-dark shift microelectrode technique to variations in biomass at the tip of the oxygen microelectrode. Especially in the presence of very motile populations of phototrophs this complicates the interpretation of P vs I curves at distinct depths as both the photosynthetic activity and the distribution of the phototrophs might change as a function of irradiance (see e.g. Kühl et al. 1996). In this study we investigated, however, a cyanobacterial mat dominated by immotile unicellular *Aphanothece* sp. embedded in a dense polymer matrix and we did not observe any significant changes in mat structure due to migration. Combination of microscale photosynthesis measurements with a non-invasive method for determining microscale biomass distribution would allow a correction for changes in biomass distribution. Such a method could be based on pigment distribution as determined from spectral measurements of reflected light (Kühl et al. 1994b, Bebout & Garcia-Pichel 1995) or fluorescence (Schreiber et al. 1996, Kühl unpubl. results) with fiber-optic radiance microprobes.

Fine-scale measurement of E_0(PAR) is an important prerequisite for understanding light regulation of photosynthesis in dense light absorbing and scattering systems. The present system for microscale measurements of E_0(PAR) represents a simple and robust technique to measure PAR down to <1 µmol photons m^{-2} s^{-1} at high spatial resolution in the laboratory or directly in the field. In combination with oxygen microsensors it is now possible to study photosynthetic adaptation to PAR at different locations in stratified microbenthic communities like microbial mats, photosynthetic sediments, and biofilms with minimal disturbance of the community (e.g. Kühl et al. 1996, Ploug 1996). Besides its obvious usability in these benthic communities, the presented system may be useful in numerous other aquatic systems where fine-scale PAR measurements are necessary, e.g. in filamentous green algal mats or other macroalgal assemblages, aquatic macrophytes, marine and freshwater aggregates, or in photosynthetic symbiotic consortia like e.g. corals (Kühl et al. 1995) and foraminifera.

Acknowledgements. We thank Poul Erik Mikkelsen and Einar Larsen for help with the development of mechanical and optoelectrical parts of the light meter. Bo Barker Jørgensen, C.R. Booth and Thomas Richter are thanked for discussions and suggestions. Yehuda Cohen, Yael Helman, and Avram Fish are thanked for their help and for providing lab facilities at the Interuniversity Institute, Eilat, Israel. Support was from the Red Sea Research Program, Project E - 'Microbial activities in hypersaline interfaces controlling nutrient fluxes', financed by the German Ministry for Research and Development (BMBF), and a grant from the Center for Freshwater Research under the Danish Strategic Environmental Research Program (awarded to N.P.R.).

LITERATURE CITED

Baumert H (1996) On the theory of photosynthesis and growth in phytoplankton. Part I: Light limitation and constant temperature. Int Rev Ges Hydrobiol 81:109–139

Bebout BM, Garcia-Pichel F (1995) UVB-induced vertical migration of cyanobacteria in a microbial mat. Appl Environ Microbiol 61:4215–4222

Biggs WW. Radiation measurement. Application note from LiCor Inc, Lincoln, NE, p 1–6

Biggs WW, Edison AR, Eastin KW, Brown KW, Maranville JW, Clegg MD (1971) Photosynthesis light sensor and meter. Ecology 52:125–131

Booth CR (1976) The design and evaluation of a measurement system for photosynthetically active quantum scalar irradiance. Limnol Oceanogr 21:326–336

Dodds WK (1992) A modified fiber-optic light microprobe to measure spherically integrated photosynthetic photon flux density: characterisation of periphyton photosynthesis-irradiance patterns. Limnol Oceanogr 37:871–878

Eilers PHC, Peeters JCH (1989) A model for the relationship between light intensity and the rate of photosynthesis in phytoplankton. Ecol Model 42:199–215

Garcia-Pichel F (1995) A scalar irradiance fiber-optic microprobe for the measurement of ultraviolet radiation at high spatial resolution. Photochem Photobiol 61:248–254

Geider RJ, Osborne BA (1992) Algal photosynthesis: the measurement of algal gas exchange. Chapman & Hall, New York

Højerslev NK (1981) Daylight measurements appropriate for photosynthetic studies in natural sea waters. J Cons Int Explor Mer 38:131–146

Jassby AD, Platt T (1976) Mathematical formulation of the relationship between photosynthesis and light for phytoplankton. Limnol Oceanogr 21:540–547

Jerlov NG, Nygaard K (1969) A quanta and energy meter for photosynthesis studies. Rep Inst Fysisk Oceanogr, Copenhagen 10:1–29

Jewson DH, Talling JF, Dring MJ, Tilzer MM, Heaney SI, Cunningham C (1984) Measurement of photosynthetically available radiation in freshwater: comparative tests of some current instruments used in studies of primary production. J Plankton Res 6:259–273

Jørgensen BB, Des Marais DJ (1986) A simple fiber-optic microprobe for high resolution light measurements: application in marine sediment. Limnol Oceanogr 31:1376–1383

Jørgensen BB, Des Marais DJ (1988) Optical properties of benthic photosynthetic communities: fiber-optic studies of cyanobacterial mats. Limnol Oceanogr 33:99–113

Kazarinova-Fukshansky N, Fukshansky L, Kühl M, Jørgensen BB (1996) Theory of equidistant three-dimensional radiance measurements with optical microprobes. Appl Optics 35:65–73

Kirk JTO (1994) Light and photosynthesis in aquatic ecosystems, 2nd edn. Cambridge University Press, Cambridge

Kühl M, Cohen Y, Dalsgaard T, Jørgensen BB, Revsbech NP (1995) Microenvironment and photosynthesis of zooxanthellae in scleractinian corals studied with microsensors for O_2, pH and light. Mar Ecol Prog Ser 117:159–172

Kühl M, Glud RN, Ploug H, Ramsing NB (1996) Microenvironmental control of photosynthesis and photosynthesis-coupled respiration in an epilithic cyanobacterial biofilm. J Phycol 32(5):799–812

Kühl M, Jørgensen BB (1992) Spectral light measurements in microbenthic phototrophic communities with a fiber-optic microprobe coupled to a sensitive diode array detector. Limnol Oceanogr 37:1813–1823

Kühl M, Jørgensen BB (1994) The light field of microbenthic communities: radiance distribution and microscale optics of sandy coastal sediments. Limnol Oceanogr 39: 1368–1398

Kühl M, Lassen C, Jørgensen BB (1994a) Light penetration and light intensity in sandy marine sediments measured with irradiance and scalar irradiance fiber-optic microprobes. Mar Ecol Prog Ser 105:139–148

Kühl M, Lassen C, Jørgensen BB (1994b) Optical properties of microbial mats: light measurements with fiber-optic microprobes. In: Stal LJ, Caumette P (eds) Microbial mats: Structure, development and environmental significance. NATO ASI Ser G, Vol 35. Springer, Berlin, p 149–167

Lassen C, Jørgensen BB (1994) A fiber-optic irradiance microsensor (cosine collector): application for *in situ* measurements of absorption coefficients in sediments and microbial mats. FEMS Microbiol Ecol 15:321–336

Lassen C, Ploug H, Jørgensen BB (1992a) A fibre-optic scalar irradiance microsensor: application for spectral light measurements in sediments. FEMS Microbiol Ecol 86:247–254

Lassen C, Ploug H, Jørgensen BB (1992b) Microalgal photosynthesis and spectral irradiance in coastal marine sediments of Limfjorden, Denmark. Limnol Oceanogr 37: 760–772

Lassen C, de Wit R, Lorentzen J, Revsbech NP (1994) Light and photosynthesis. In: Caumette P (ed) CLEAN progress report. The Commission of the European Union, Brussels

Platt T, Gallegos CL, Harrison WG (1980) Photoinhibition of photosynthesis in natural assemblages of marine phytoplankton. J Mar Res 38: 687–701

Ploug H (1996) Light and photosynthesis in dense populations of microalgae. PhD thesis, University of Aarhus

Ploug H, Lassen C, Jørgensen BB (1993) Action spectra of microalgal photosynthesis and depth distribution of spectral scalar irradiance in a coastal marine sediment of Limfjorden, Denmark. FEMS Microbiol Ecol 12:69–78

Revsbech NP (1989) An oxygen microelectrode with a guard cathode. Limnol Oceanogr 34:474–478

Revsbech NP (1994) Analysis of microbial mats by use of electrochemical microsensors: recent advances. In: Stal LJ, Caumette P (eds) Microbial mats: structure, development and environmental significance. NATO ASI Ser G, Vol 35. Springer, Berlin, p 135–147

Revsbech NP, Jørgensen BB (1983) Photosynthesis of benthic microflora measured with high spatial resolution by the oxygen microprofile method: capabilities and limitations of the method. Limnol Oceanogr 28:749–756

Schreiber U, Kühl M, Klimant I, Reising H (1996) Measurement of chlorophyll fluorescence within leaves using a modified PAM fluorometer with a fiber-optic microprobe. Photosynth Res 47:103–109

Smith RC, Wilson WH (1972) Photon scalar irradiance. Appl Optics 11:934–938

Spitzer D, Wernand MR (1979) Photon scalar irradiance meter. Appl Optics 18:1698–1700

Webb WLM, Newton M, Starr D (1974) Carbon dioxide exchange of *Alnus rubra*: a mathematical model. Oecologia 17:281–291

Responsible Subject Editor: Henry Blackburn, Aarhus, Denmark

Manuscript received: December 6, 1996
Revised version accepted: April 16, 1997